ISSN No: -2456-2165 https://doi.org/10.38124/ijisrt/25oct1118

Synthesis and Characterization of Calcium Silicate Hydrate from Oyster Shell and De-Aluminated Metakaolin Based Sodium Silicate Via Sol Gel Precipitation Method at Ambient Temperature

A. Abandoh[1*]; A. C. K. Amuzu[1]; B. Puzer[1]; F. J. K. Adzabe[2]; S. Anane[3]; L. K. Labik[1]; I. Nkrumah[1]; E. K. K. Abavare[1]; B. Kwakye-Awuah[1]

[1]Department of Physics, Kwame Nkrumah University of Science and Technology, Kumasi, Ghana.
[2]Department of Mechanical Engineering, Kumasi Technical University, Kumasi, Ghana.
[3] Department of Programs, Ghana Investment for Electronic Communications, Kumasi, Ghana.

Corresponding Author: A. Abandoh[1*]

Publication Date: 2025/11/03

Abstract: This study employed a facile sol-gel precipitation method to synthesize calcium silicate hydrate (CSH) at room temperature using oyster shell-derived calcium nitrate and de-aluminated metakaolin-derived sodium silicate as sustainable precursors. The evolution of CSH gel from an initial stoichiometric Ca/Si molar ratio of 0.68 into crystalline phases was investigated over different aging periods (1, 3, 7, and 14 days). The microstructural characteristics of the synthesized CSH were comprehensively analyzed using Fourier transform infrared spectroscopy (FTIR), powder X-ray diffraction (XRD), X-ray fluorescence spectroscopy (XRF), energy-dispersive X-ray spectroscopy (EDX), thermogravimetric analysis (TGA), and scanning electron microscopy (SEM). XRF analysis revealed a progressive increase in Ca/Si ratio from 0.63 (Day 1) to 0.88 (Day 14), indicating enhanced calcium incorporation during aging. FTIR spectra confirmed the formation of hydrated silicates through characteristic functional groups (O–H, Si–O, and Si–O(Ca)), with band intensity evolution suggesting increased silicate chain polymerization over time. XRD patterns confirmed tobermorite-like crystalline phases at extended aging periods, correlating with improved structural ordering. TGA analysis revealed distinct thermal decomposition profiles attributed to adsorbed water loss, CSH phase dehydration, and decarbonation. SEM micrographs of 14-day aged CSH exhibited dense, fibrous morphology characteristic of well-developed CSH phases, while EDX analysis confirmed silicon and calcium as the predominant elements, corroborating XRF findings. Prolonged aging enhanced crystallinity, calcium content, and polymerization degree, aligning with properties reported for high-performance cementitious materials. These results demonstrated the viability of utilizing oyster shells and de-aluminated metakaolin as eco-friendly precursors for CSH synthesis. This study highlights the potential for valorizing dealuminated metakaolin and oyster shells into advanced materials for sustainable construction applications; and offers promising pathway for reducing environmental wastes while contributing to greener construction material development. Future research should focus on optimizing synthesis parameters and evaluating the mechanical and durability properties of CSH in composite systems.

Keywords: *Calcium Silicate Hydrate (CSH); C/S Ratio; Dealuminated Metakaolin, Period, Oyster-Shell.*

How to Cite: A. Abandoh; A. C. K. Amuzu; B. Puzer; F. J. K. Adzabe; S. Anane; L. K. Labik; I. Nkrumah; E. K. K. Abavare; B. Kwakye-Awuah (2025). Synthesis and Characterization of Calcium Silicate Hydrate from Oyster Shell and De-Aluminated Metakaolin Based Sodium Silicate Via Sol Gel Precipitation Method at Ambient Temperature. *International Journal of Innovative Science and Research Technology*,10(10), 2133-2142. https://doi.org/10.38124/ijisrt/25oct1118

I. INTRODUCTION

Calcium silicate hydrate (CSH) is a key component which mostly forms during the hydration of ordinary Portland cementitious masonry units such as sandcrete blocks and concrete; and plays a crucial role in determining their strength, durability, and overall performance. As the principal hydrate phase in the masonry units, CSH is responsible for binding the aggregates together with the cement particles thereby providing the masonry units with desirable mechanical properties [1]. This principal product of Ordinary Portland Cement (OPC), according to [1], makes up

ISSN No: -2456-2165 https://doi.org/10.38124/ijisrt/25oct1118

to 60 % by volume of harden cement paste thus making the OPC the most widely used contemporary material in the construction industry after water [2]. The quest to improve the early strength development in OPC masonry units coupled with some other equally important applications has driven the interest in research works toward the synthesis of this versatile material with focus on enhancing its structure, composition, and reactivity which have significant impact on the properties of the masonry units. This pursuit is also critical for mitigating the environmental impact of concrete production by lowering the amount of cement needed, thus minimizing the carbon footprint associated with cement manufacturing. As such literature is replete with works on various methods of synthesis of the CSH from different calcium and silicate based precursors in recent years [1, 3-13]. Literature has shown that synthesis techniques and conditions have enormous effects on the phase composition, crystal structure and morphology of synthetic calcium silicate hydrate (CSH) more than its precursors.

Reference [14], reported the synthesis CSH using calcium oxide and colloidal silica suspension under nitrogenous condition. Even though the authors varied the C/S ratio in a range of 0.8 – 3.0 in the initial gel formation, they did not report the final C/S ratio of the synthetic CSH because it was not measured. The obtained CSH gel although made with a low H_2O/CaO ratio of 2, was used for extended leaching tests with no solid state chemical or mechanical characterization performed.

Reference [15], in the attempt to investigate the solubility and structure of CSH, synthesised CSH via a double decomposition technique in which CSH was precipitated from aqueous sodium silicate and calcium nitrate in nitrogen atmosphere and reported the synthesised CSH had C/S ratio of 1.4 with some trace of residual alkali. However, the reaction temperature and the type of CSH phase obtained were not stated in this study.

In a conventional and microwave assisted hydrothermal techniques, [16] synthesized 11 Å tobermorite using combination of different silicon sources such as borosilicate glass, silicic acid and quartz in a reaction with calcium hydroxide at initial C/S molar ratios ranging from 0.36 – 1.78 with focus on investigating the effect of silicon precursor, reaction time and reaction technique on the formation of 11 Å tobermorite. The reaction temperature for both conventional and microwave assisted hydrothermal reactions was 200 ^oC and reaction times of 7 days and 8 hours respectively for the conventional and microwave assisted hydrothermal reactions. Their XRD and TEM analyses revealed that all silicon precursors were ideal for the synthesis of 11 Å tobermorite. Notwithstanding, all products from the microwave assisted method exhibited poor crystallinity compared to those synthesised by the conventional method. According to the authors, maximum yield of tobermorite was obtained within 3 days of reaction time in the conventional method. They have also demonstrated the effectiveness of starting C/S ratio on the phase purity of the synthetic product. They observed that starting C/S ratio of up to 0.6 resulted in almost pure tobermorite phase, whereas at a ratio of up to 0.89, another C – S – H phase known as xonotlite formed alongside the tobermorite phase. A mixture of calcium silicate and calcium silicate hydrate was observed for C/S ratio of 1.78.

In similar vein, [9] investigated the effect of hydrothermal reaction conditions on the formation of crystalline calcium silicate such as tobermorite and xonotlite. The starting materials employed in their investigation were calcium oxide, and silicon from three different types of siliceous materials such as quartz, nano-silica, and diatomite. The synthesis parameters considered in this study include: water to solid weight ratio (10), C/S molar ratios (0.83 and 1.0) reaction temperatures (120 and 185 ^oC), reaction time (1-24 hours), and heat rate (0.75 and 1.70 ^oC/min). The samples herein obtained were characterized based on XRD and the authors, found that nano-silica powder were more suitable for synthesis of pure amorphous CSH, whereas crystalline siliceous materials may be good for producing crystalline CSH. They also observed that the formation of tobermorite and xonotlite were largely influenced by the temperature and heating rate during hydrothermal reaction.

General observations from literature suggest that, aside synthesis parameters such as Ca/Si ratio, pH, temperature, and reaction time, maintaining a nitrogenous environment during synthesis of calcium silicate hydrate remains the most important condition necessary for the development of a crystalline calcium silicate hydrate of any phase without any ancillary phase such as calcite. Thus reaction vessels are mostly kept under inert nitrogen atmosphere during synthesis to avoid the formation of calcite [1,7,10,17]. This does not only make the synthesis process rather complex but, also increase the cost of production since a nitrogen gas must be passed through the reaction vessel for several hours or days.

In order to address this challenge, the attempt was made in this research work to synthesize calcium silicate hydrate using in-situ nitrogenous liquid phase reaction technique which eliminate the use of nitrogen gas. This novel technique comes in handy, relatively simple and cost effective because the basic elements of the calcium silicate hydrate are obtained from natural precursors such as oyster shell and kaolin.

II. MATERIALS AND METHODS

- *Reagents*

Sulphuric acid (H_2SO_4, 95%), Nitric acid (HNO_3, 99%), sodium hydroxide pellets (NaOH, 99%), and ethanol (95%) were purchased from Sigma-Aldrich, UK. All chemicals were used without any further purification.

- *Precursors*

Kaolin was obtained, taken through beneficiation process, calcined and de-aluminated to obtain an amorphous silica precursor whose chemical constituent was analyzed and presented in Table 4.1. Oyster shell was sourced from local market, washed, dried, ground and sieved (150 μm) to obtain a fine powdered calcium carbonate sample with uniform particle sizes. The powdered sample was then heat treated in

ISSN No: -2456-2165 https://doi.org/10.38124/ijisrt/25oct1118

a muffle furnace at 450 °C for 2 hours, after which the furnace was turned off and the sample allowed to cool to ambient temperature, recovered thereafter and stored in a sealed container. Its chemical constituent was analyzed and the result also presented in Table 4.1.

➢ *Methods*

- *Preparation of Sodium Metasilicate Na_2SiO_3*

Sodium metasilicate of SiO_2/Na_2O modulus of 1.5 with 24 wt% SiO_2 and 60 wt% H_2O was prepared from the amorphous silica according to protocol described by [18] "unpublished" with slight modification. This was done by weighing simultaneously 100.0 g of the amorphous silica and 66.7 g of sodium hydroxide into a 1000 ml plastic beaker and mixed thoroughly. 250.1 g of distilled water was added gently to the mixture which resulted in an exothermic reaction. The exothermic reaction was allowed to complete and the mixture transferred into a 500 ml Teflon bottle, well capped and placed in an electric oven at 150 °C for 90 min. The bottle was removed after the reaction time, cooled to about 90 °C. The as-prepared solution was topped up 500 ml and filtered under vacuum to obtain a clear solution which was transferred into a clean plastic container and ready for use. Equation 3.1 describes the chemical reaction which occurred in this process.

$$SiO_{2(s)} + 2NaOH_{(aq)} \rightarrow Na_2SiO_3 + H_2O \quad (3.1)$$

- *Preparation of Calcium Nitrate ($Ca(NO_3)_2$)*

The powdered calcium carbonate from the oyster shell was first converted into calcium hydroxide. This was done by weighing 200.2 g of the powdered calcium carbonate into 1000 ml beaker to which 160.0 g of sodium hydroxide was added and mixed to obtain a uniform mixture. Subsequently, 140 ml of distilled water was added gently to the mixture to facilitate the reaction. The reaction mixture was stirred at 90 rpm using magnetic stirrer at 55 °C for 90 min. The calcium hydroxide was then filtered washed with distilled water, dried, ground into fine powder. A 2 Molar $Ca(NO_3)_2$ stock solution was then prepared from the prepared $Ca(OH)_2$ powder and the nitric acid. 148.19 g of $Ca(OH)_2$ was weighed into a beaker and 252.05 g of nitric acid (4 mol/dm^3) weighed and poured gently onto the $Ca(OH)_2$ in the beaker while stirring manually with Teflon rod. The mixture was further stirred at 120 rpm on a magnetic stirrer at 90 °C for 60 min to obtain clear solution. The solution was then transferred into 1000 ml volumetric flask and the volume adjusted with distilled water to 1 liter to obtain a 2 M $Ca(NO_3)_2$ stock solution ready for use. Equations 3.2 and 3.3 describe the reactions involved in this process.

$$CaCO_3 + 2NaOH \rightarrow Ca(OH)_2 + Na_2CO_3 \quad (3.2)$$

$$Ca(OH)_2 + 2HNO_3 \rightarrow Ca(NO_3)_2 + 2H_2O \quad (3.3)$$

- *Synthesis Calcium Silicate Hydrate*

Calcium silicate hydrate gel was prepared from the sodium silicate and calcium nitrate solutions using a Ca/Si molar ratio of 1. The gel was obtained by mixing 1.0 M of $Ca(NO_3)_2$ dropwise with 1.0 M of Na_2SiO_3 in a litre beaker under stirring condition using magnetic stirrer at 100 rpm and increased to 150 rpm as the gel formed. 0.5 M of $NaNO_3$ solution was prepared and added to the gel to ensure a rich nitrogenous environment for the development the CSH. The gel was homogenized by stirring for 2 Hours at ambient temperature. It was then transferred into equal volumes of 4 four Teflon bottles which were well capped and aged for 1, 3, 7, and 14 days to crystallize the CSH under ambient conditions thereby mimicking how the CSH develop in OPC masonry units. After each of the induction period, the crystallized product was recovered, filtered, washed with an aliquot of 1:1 aqueous ethanol solution then thoroughly washed with distilled water, dried, ground and stored in Ziploc bag. The primary reaction between sodium silicate and calcium nitrate can be represented as:

$$Ca(NO_3)_2 + Na_2SiO_3 + xH_2O \rightarrow CaSiO_3.xH_2O + 2NaNO_3 \quad (3.4)$$

III. CHARACTERIZATION

➢ *Elemental Constituents of Precursors and As-Synthesized CSH*

De-aluminated metakaolin, Oyster shell powder, calcium hydroxide, and as-synthesized CSH samples were analysed for their elemental composition using the Rigaku NEX CG XRF at the Earth Science Department, University of Ghana.

Table 1 Chemical Constituents of CSH Precursors

Sample	Oxide /wt%						
	SiO_2	CaO	SO_3	Al_2O_3	ZrO_2	MgO	Others
De-aluminated metakaolin	98.30	ND	0.77	0.64	0.14	ND	0.15
Oyster shell	2.90	94.24	0.34	0.33	0.45	1.45	1.01
Calcium hydroxide	0.02	98.65	0.07	0.36	0.45	0.32	0.13

➢ *Microstructure Characteristics of CSH Samples*

The microstructural development of CSH under different ageing conditions was characterized by X-ray diffraction (XRD, EMPYREAN/0000000011136412, Cu Kα radiation, λ of Kα1 =1.540 6 Å). The rate of scanning was 2 °C/min with 2θ ranging 5 to 70° and a step size of 0.02°. The device operated at 40 mA and 45 kV for phase analysis using the Bragg – Brentano geometry.

The functional groups of the developed CSH were also analyzed using Fourier transform infrared spectroscopy (FTIR) (Perkin-Elmer Spectrum 100). TGA/DSC (NETSZCH STA 449 F1, Jupiter) analyses were also

ISSN No: -2456-2165 https://doi.org/10.38124/ijisrt/25oct1118

conducted on the samples to examine their thermal properties.

Scanning electron microscopy (SEM, Hitachi S4800, Japan) equipped with energy dispersive X-ray spectrometer (EDX) with nominal electron beam voltages of 15 kV, was used to examine the surface morphology and elemental constituent of Day 14 sample.

IV. RESULTS AND DISCUSSION

➢ *Results*

- *XRF Analysis of Starting Materials and As-Synthesized CSH*

The results of the chemical constituents of the de-aluminated metakaolin, oyster shell, and calcium hydroxide, as determined by XRF analysis, are presented in Table 1. As shown in Table 1, the de-aluminated metakaolin was primarily composed of SiO_2 (98.30%), with minor amounts of other oxides, including CaO, SO_3, Al_2O_3, TiO_2, Fe_2O_3, ZrO_2, and MgO. The de-aluminated metakaolin, characterized by its exceptionally high silica content, was found to be a suitable precursor for the production of sodium metasilicate, a crucial reagent in the synthesis of calcium silicate hydrate (CSH). On the other hand, the XRF analysis revealed that the oyster shell was predominantly composed of CaO (94.24%), with significant amounts of SiO_2 (2.90%) and trace amounts of other oxides. This made it a suitable material for the production of calcium hydroxide.

The XRF analysis of the calcium hydroxide revealed that it has a higher CaO content (approximately 99.00%) compared to the oyster shell from which it was derived. The analysis indicated that all the raw materials possessed the characteristic constituent elements in sufficiently high percentages, making them suitable for the synthesis of CSH.

The chemical composition of the as-synthesized CSH samples for different induction periods was investigated using XRF, and the results are presented in Table 2. As indicated in Table 2, the as-synthesized products were primarily composed of silica and calcium oxide, along with trace amounts of metallic oxides and sulfate. However, the SiO_2 content decreased progressively in the samples from 59.60% on Day 1 to 53.10% by Day 14, accompanied by a notable increase in CaO from 37.45% to 46.50%. Furthermore, minimal changes were observed in the concentrations of Al_2O_3, ZrO_2, and Na_2O over time, whereas SO_3 exhibited a slight decrease by Day 7 (0.39%) before disappearing entirely by Day 14. These compositional shifts reflect the crystallization and chemical transformations that occurred within the as-synthesized CSH products. Analysis of the XRF results of as-synthesised CSHs revealed the ratio of CaO to SiO_2 increased steadily from 0.63 on Day 1 to 0.88 on Day 14. This trend indicated a relative enrichment of calcium oxide in the structural growth of the CSH over time, likely due to ongoing crystallization reactions, which consumed SiO_2 and increased the CaO content as the crystal structure of the CSH matured.

- *XRD Analysis of the As-Synthesized CSH*

The phase evolution of the as-synthesized CSH was studied using X-ray powder diffraction (XRD) with a Bragg-Brentano θ-2θ geometry to elucidate the crystal structure and phase composition of the samples. The diffractograms from the analysis of CSH samples synthesized at various induction periods presented in Fig. 1 below exhibit distinct changes indicative of phase evolution over time. The diffraction pattern for earliest age (Day 1) showed nitratine (36.8%), calcite (27.0%) and Tobermorite (26.3 %) as the major phases with portlandite (9.9%) being the only minor phase in the diffraction pattern.

Comparatively, tobermorite peaks in this pattern are weaker compared to nitratine and calcite, suggesting limited formation of the CSH phase.

However, spectral for induction period (Day 3) shows tobermorite (70.2%) phase increased significantly becoming the dominant phase with intense peaks, indicating active conversion of precursors into the CSH phase.

Table 2 Chemical Composition of As-Synthesised CSH

Sample	Oxide /wt%							Ca/Si Ratio
	SiO_2	CaO	SO_3	Al_2O_3	ZrO_2	Na_2O	Others	
CSH – Day 1	59.60	37.45	0.43	0.08	0.43	1.82	0.21	0.63
CSH – Day 3	58.45	38.60	0.43	0.08	0.43	1.82	0.21	0.66
CSH – Day 7	56.78	39.64	0.39	0.35	0.28	1.76	0.71	0.70
CSH – Day 14	53.10	46.50	0.00	0.00	0.35	0.01	0.04	0.88

Calcite (29.8%) remains a notable secondary phase, likely due to carbonation processes during the synthesis. Nevertheless, other phases from Day 1, such as nitratine and portlandite, were no longer observed, reflecting the progression of the reaction. Similarly, as the induction period progressed (Day 7), the tobermorite (78.5%) phase became more dominant with even more intense peaks, confirming further crystallization of the CSH phase. Calcite phase also decreased to 21.5% with reduced peak intensity, suggesting reduction in carbonation as the tobermorite phase stabilized. Furthermore, the diffraction pattern for induction period (Day 14) reveals that the tobermorite phase (95.3%) emerged as the predominant crystalline phase, characterized by sharp and intense diffraction peaks suggesting complete evolution of a well-crystallized CSH structure with calcite (4.7%) as a minor phase with relatively less intense peak. It is to be noted that these results compare well with those reported in literature [11,12,13].

ISSN No: -2456-2165 https://doi.org/10.38124/ijisrt/25oct1118

General observation from the XRD patterns of the CSH suggests that as the induction period progressed from Day 1 to Day 14, there was a distinct transformation from a multiphase system (nitration, calcite, portlandite, and tobermorite) to a predominantly single-phase system dominated by tobermorite. This demonstrated the crystallization of the CSH structure over time, with decreasing byproducts and increasing crystallinity.

- *FTIR Analysis of the As-Synthesized CSH*

The functional groups in the structural frame work of the as-synthesised CSH were studied using FTIR and the results presented in Fig. 2 below show their characteristics bands. The Figure reveals that the characteristics bands were influenced by the induction periods as slight variations were observed in all samples. Vibrations bands at 3560 cm^{-1} signifying the presence of hydroxyl functional groups were observed for all samples due to the presence of surface or adsorbed water showing the porous nature of the products. Carbonate functional groups were also observed in Day 1, Day 3 and Day 7 at wavenumber but, were largely absent in Day 14 sample. Silanol groups with vibration mode at 1050 – 980 cm^{-1} were however observed in all the samples synthesised at the different induction period.

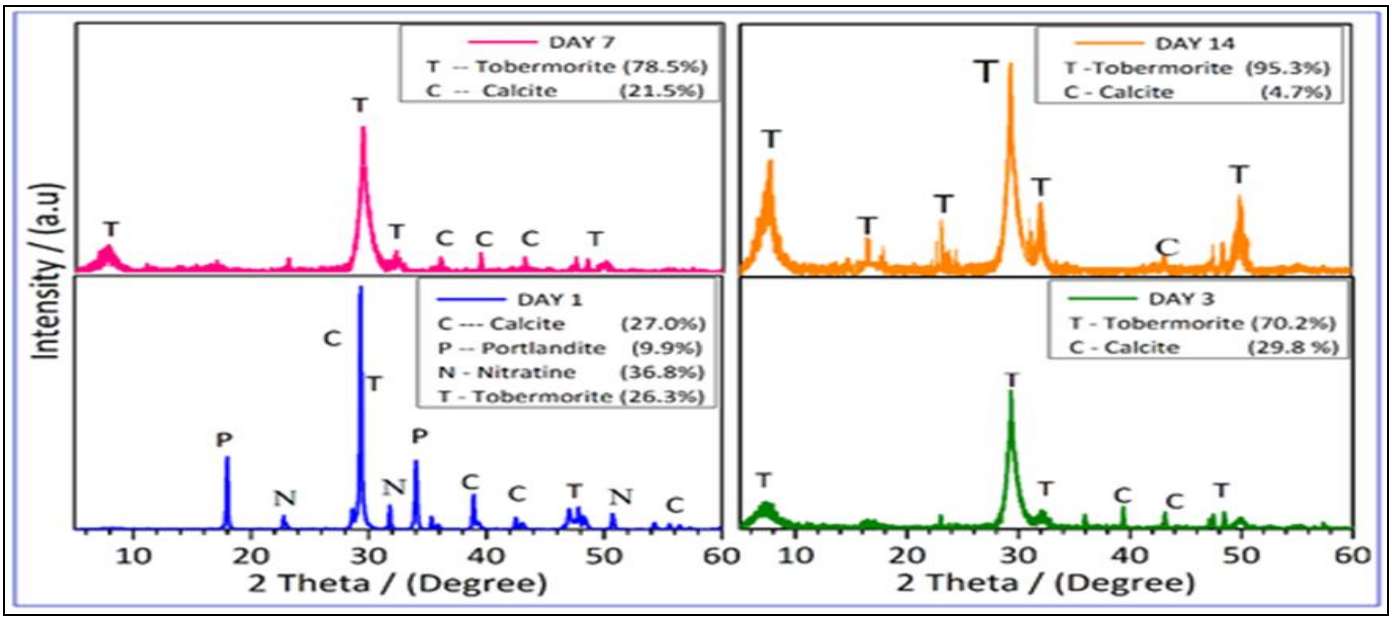

Fig 1 XRD Spectrum of the As-Synthesized CSH Showing Evolution of Tobermorite.

These functional groups were congruous with those reported in literature [6,19]. The FTIR spectra demonstrate a transition from a hydrated, carbonate-rich early phase (Day 1) to a predominantly crystalline, carbonate-free CSH structure by Day 14. Over time, the silicate network became more polymerized, and the material exhibited reduced water and carbonate content, aligning with the progression of crystallization reactions and phase stabilization.

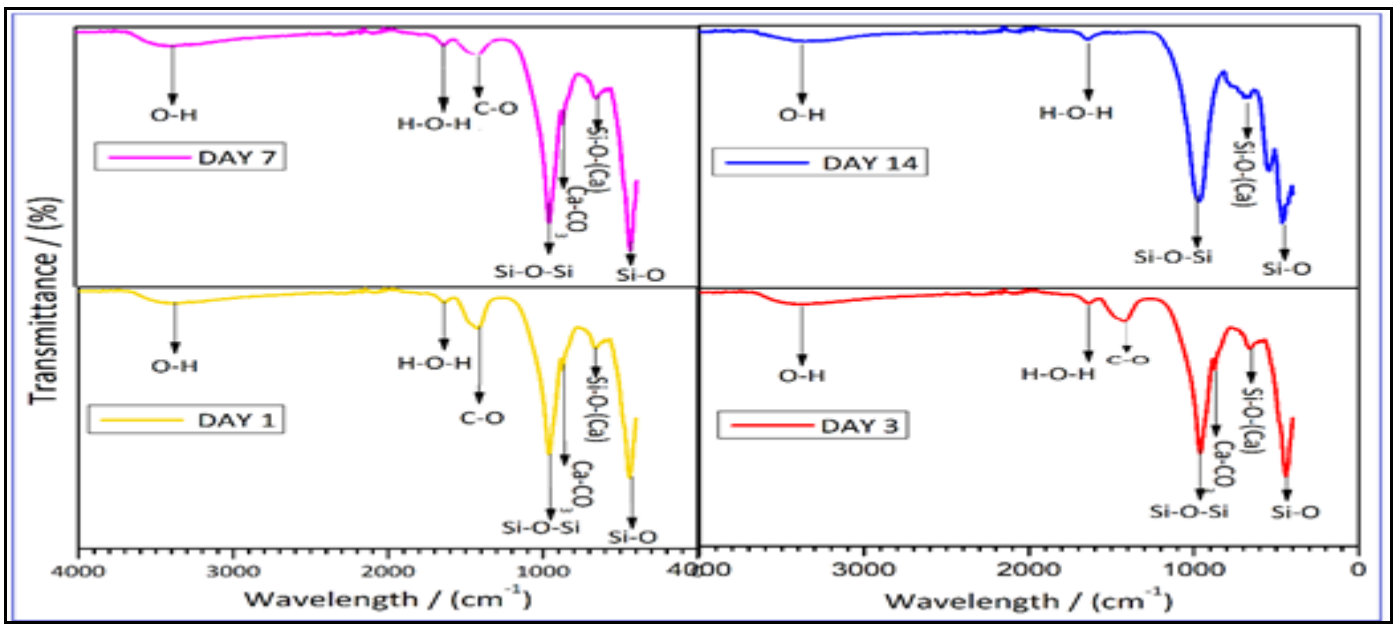

Fig 2 FTIR Spectrum of the As-Synthesized CSH Showing Functional Groups.

ISSN No: -2456-2165 https://doi.org/10.38124/ijisrt/25oct1118

- *TGA/DSC Analyses of the As-Synthesized CSH*

The thermogravimetric analysis (TGA) and differential scanning calorimetry (DSC) curves of calcium silicate hydrate (CSH) conducted within a temperature range of 30 – 1000 °C are presented in Fig. 3 below.

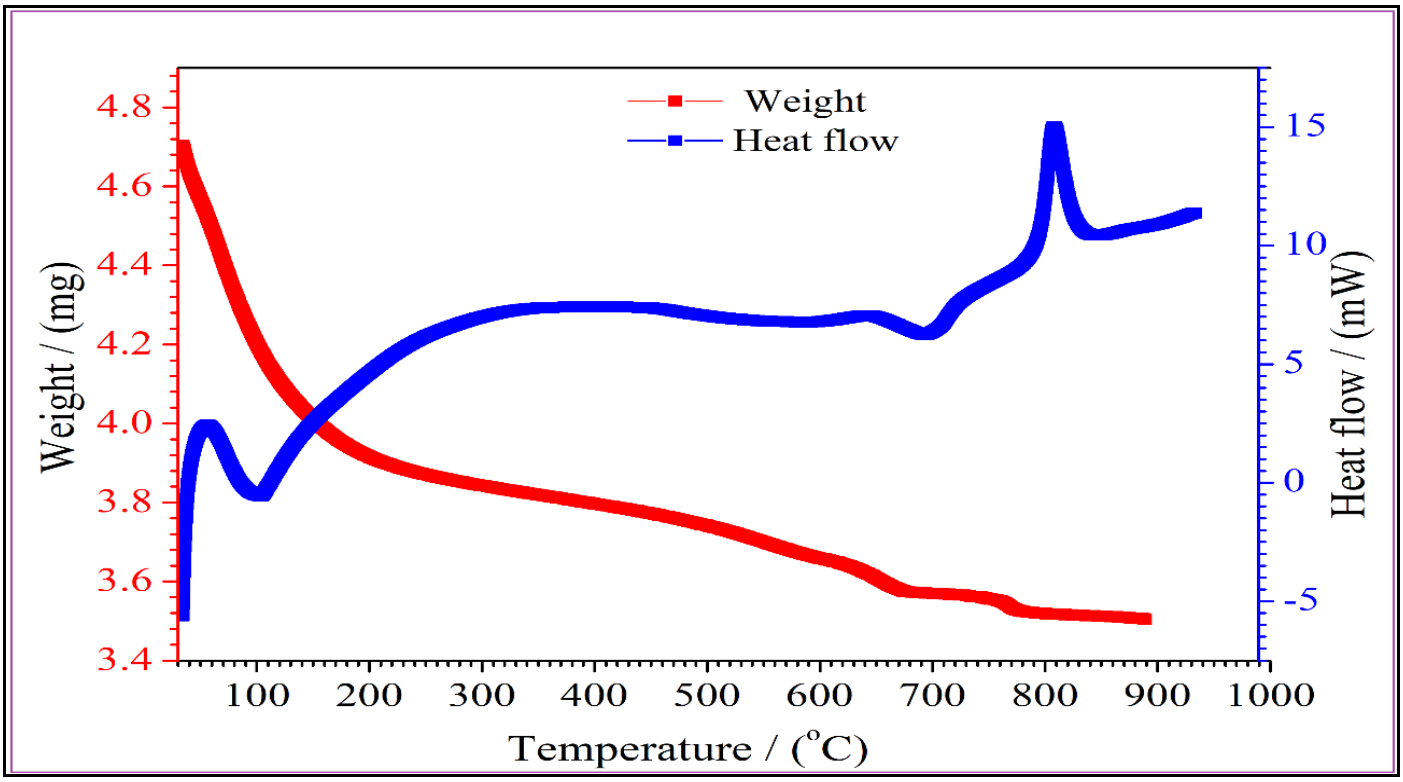

Fig 3 TGA/DSC Thermograms of Day 14 As-Synthesized CSH

The TGA curve (red line) illustrated the weight loss as a function of temperature, while the DSC curve (blue line) represents the associated heat flow characteristics of the CSH sample. The TGA curve showed a pronounced weight loss was observed below 200°C, attributed to the release of physically adsorbed water and inter-layer water from the CSH structure [10]. However, the weight loss continued gradually in the temperature range of 200–600°C, likely corresponding to the loss molecular water or CO_2 from impurity phase such as calcium carbonate [10,12]. Moreover, beyond 800°C, the weight stabilized, indicating the near-complete thermal decomposition or transformation of the CSH material. The DSC curve also showed an endothermic peak in the range of 100–200°C, associated with the dehydration of physically adsorbed and inter-layer water. A broad exothermic signal is observed above 600°C, which may be attributed to the recrystallization of calcium silicate phases or the formation of thermally stable phases, such as wollastonite [12, 20, 21].

The SEM micrograph and EDX spectrum of the Day 14 as-synthesised CSH are presented in Fig. 4 below. The SEM micrograph shows the sample exhibited characteristic morphology of calcium silicate hydrate (CSH), specifically resembling a fibrous and interlaced structure, which is typical of tobermorite-like phases. It can be observed that the micrograph prominently displays elongated fibrous particles intertwined to form a network-like structure. This interlaced arrangement is a key feature of tobermorite [1,4], a crystalline phase of CSH, indicating its dominance presence in the sample as corroborated by the XRD diffraction pattern presented in Fig. 1.

The fibers exhibit varying lengths and widths, with a high degree of connectivity, which contributes to the structural integrity of the material. The interwoven nature of the fibers creates a robust microstructure, characteristic of hydrated calcium silicate phases like tobermorite. The porous texture is evident, with gaps and voids distributed throughout the interlaced fibrous network as evident by the TGA/DSC thermogram presented in Fig. 3. This porosity is essential for water retention and transport properties in cementitious systems. The observed fibrous morphology was consistent with the partially crystalline nature of tobermorite. This phase forms under specific conditions of hydration, typically in systems with a high calcium-to-silica ratio. The fibrous interlaced microstructure observed in the SEM micrograph aligned with the morphology of tobermorite, a crystalline calcium silicate hydrate phase often reported in hydrated cement systems [22]. This structure enhances the mechanical properties and durability of the material, consistent with its role in binding and strength development [1,23].

Furthermore, the EDX analysis of the CSH sample showed that the spectrum exhibited signals attributable to oxygen, silica, and calcium. However, intensity of the signal from oxygen, silica and calcium showed that the CSH sample had minimal secondary phase or impurities. Moreover, the strong signals from the elements suggested that the sample was mostly composed of the CSH.

ISSN No: -2456-2165 https://doi.org/10.38124/ijisrt/25oct1118

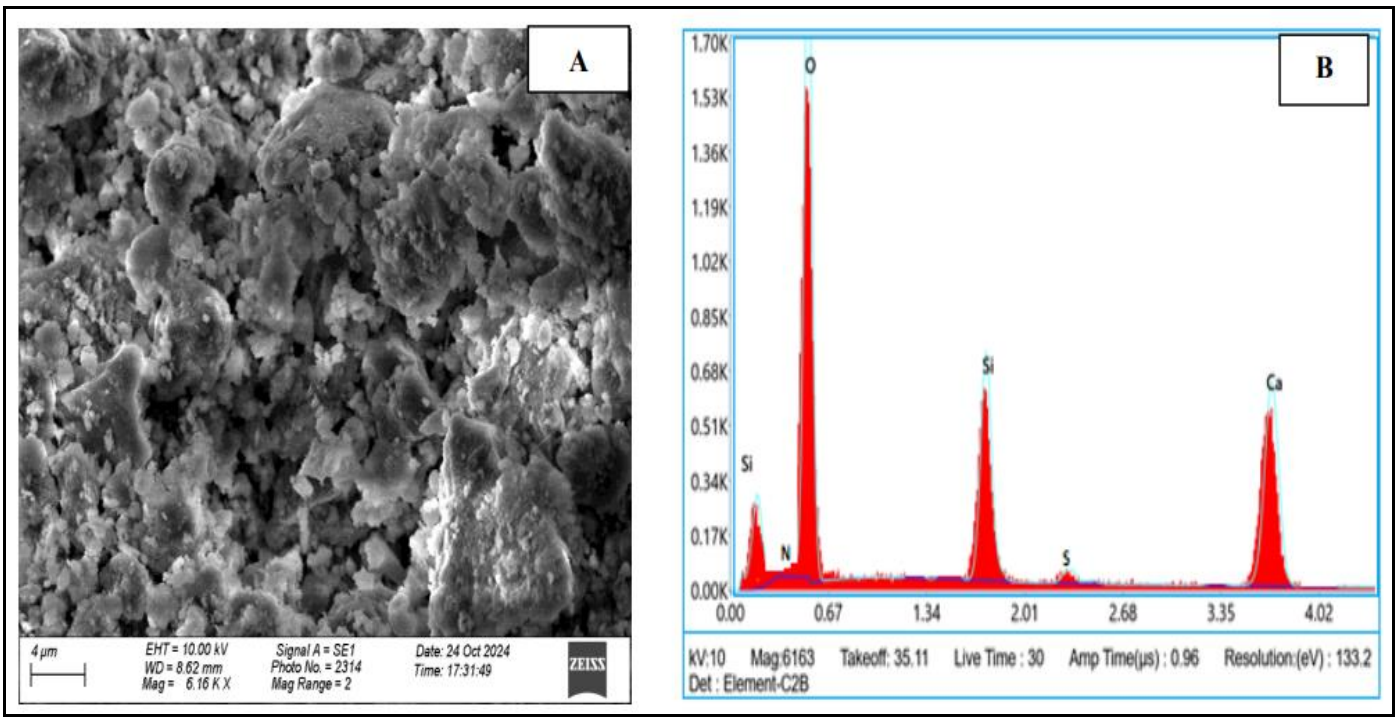

Fig 4 SEM micrograph(A) and EDX spectrum (B) of the Day 14 As-Synthesized CSH

➢ *Discussion of Results*

- *Oxide Composition of Precursors of CSH*

The XRF analysis showing the oxide compositions (wt%) of de-aluminated metakaolin, oyster shells, and calcium hydroxide presented in Table 1 revealed that these materials were candidate precursors for synthesis of the CSH. Each of these materials exhibited distinct oxide composition influenced by their source and preparation processes as revealed by the XRF analysis. De-aluminated metakaolin exhibited an extremely high content of silicon dioxide (SiO_2), with minor amounts of SO_3, Al_2O_3, and other oxides. The minimal Al_2O_3 content was an indication of effectiveness of the de-alumination process, a necessary modification to tailor its properties for specific applications, such as a silica source in synthesis of CSH and other applications. Studies reported that typical metakaolin contains SiO_2 in the range of 50–60% and Al_2O_3 around 40% [24,25,26]. The de-alumination process substantially reduced the Al_2O_3 content, leaving behind highly purified SiO_2, as observed in the XRF result which compared well with those reported in literature [27].

The analysis has also shown that oyster shell sample was predominantly composed of calcium oxide (CaO), with minor contributions from SiO_2, MgO, and trace amounts of other oxides. This high CaO content underscored its potential as a low-cost calcium source in lime production or as a raw material in cement manufacturing [28].

Similar studies reported CaO content in oyster shells ranging from 90–96%, with small amounts of SiO_2 and MgO [29,30]. However, MgO content was slightly higher in this sample compared to what was reported by [30].

The calcium hydroxide sample derived from the oyster shells exhibited higher CaO content (98.65%), with negligible SiO_2, Al_2O_3, and MgO compared to its parent material. This level of purity demonstrated the efficacy of the processing technique employed in this work. The purity makes it an ideal material for applications requiring high reactivity, such as in chemical stabilization or as a precursor in calcium silicate hydrate formation. CaO content compared well with commercial calcium hydroxide which typically exhibits CaO content in the range of 96–99% [19]. Moreover, the trace levels of impurities in this sample were within acceptable limits requisite for most industrial applications.

- *Oxide Composition of As-Synthesised CSH*

Table 2 highlighted the oxide composition (wt%) and calcium-to-silicon ratio (Ca/Si) of calcium silicate hydrate (CSH) synthesized at four different ageing periods. The analysis explored the progression of Ca/Si ratios, the accompanying changes in oxide composition, and the implications for CSH crystal structure growth into specific phase. The Ca/Si ratio progressively increased from 0.63 on Day 1 to 0.88 by Day 14, reflecting a gradual enrichment of calcium in the CSH structure over time [13]. This trend was indicative of the continued reaction between calcium ions and silicate species, leading to the formation of CSH with varying stoichiometry. Samples synthesised on Day 1 showed low Ca/Si ratio which at this stage reflected the initial incorporation of calcium into the silicate framework. The high SiO_2 content suggested a silica-rich phase, typical of early-stage CSH with a lower degree of polymerization. By Day 3 a slight increase in the Ca/Si ratio was observed, attributed to further crystallization reaction and calcium incorporation into the growing crystal structure of tobermorite phase as shown by the XRD results. A more significant rise in the Ca/Si ratio accompanied by a further reduction in SiO_2 and an increase in CaO was observed in Day 7 samples with corresponding increase in tobermorite phase. The highest Ca/Si ratio and CaO content were

ISSN No: -2456-2165 https://doi.org/10.38124/ijisrt/25oct1118

recorded in Day 14 samples, alongside a sharp decline in SiO_2. This stage represented a more crystalline phase of CSH with enhanced calcium enrichment, as reported in literature for longer ageing periods [10,14,31].

- *Phase Evolution of As-Synthesised CSH*

The phase evolution of the as-synthesized CSH with varying induction periods was studied using X-ray powder diffraction (XRD) and the diffractogram from the analysis presented in Fig. 1 showed the evolution of tobermorite CSH phase over time. Initially, at the earliest age (Day 1), the diffractogram was characterized by broad, diffuse peaks, suggesting the presence of an amorphous or poorly crystalline CSH structure [2,23]. This was typical in the early stages of nucleation and crystal growth, where rapid formation of CSH occurs with limited long-range order. As the induction period progressed to Day 3 and Day 7, the XRD patterns showed the emergence of sharper and more defined peaks. These sharper peaks corresponded to the development of well-ordered crystalline phases such as tobermorite or other layered CSH structures. The increase in peak intensity and the appearance of new diffraction lines indicated enhanced crystallinity and the growth of specific CSH polymorphs which corroborated the XRF results. Additionally, subtle shifts in peak positions were observed, reflecting changes in the calcium-to-silicon ratio and the incorporation of additional ions into the CSH lattice. By Day 14, the XRD spectrum revealed a more mature crystalline structure with prominent, high-intensity peaks corresponding to stable CSH phases. The disappearance of previously observed amorphous phases and the dominance of distinct crystalline peaks signify the completion of crystallization reactions and the stabilization of the CSH matrix. This advanced stage reflected a balanced CaO to SiO_2 ratio, as evidenced by the XRF analysis, and indicated the formation of a crystalline CSH network. In general, the XRD analysis highlights a clear progression from amorphous to crystalline phases in CSH as the induction periods extend. This phase evolution underscored the crystallization processes and maturation of the CSH structure.

- *Functional Groups in Molecular Structure of the As-Synthesised CSH*

The FTIR spectra of CSHs synthesized at different ageing periods (Day 1, Day 3, Day 7, and Day 14) presented in Fig. 2 revealed the presence of key functional groups that characterized the molecular structure of these samples. Vibrational modes for hydroxyl, carbonate, and silicate functional groups identified in these samples were largely congruous with those reported in literature [5,6,12,32]. The evolution of these groups reflected the crystal growth and polymerization processes occurring during CSH formation. The broad absorption band in 3400 – 3700 cm^{-1} corresponding to the O-H stretching vibrations of hydroxyl groups and water molecules decreased in intensity with ageing, which could be due loss of free content and increment structural order. Similarly, bending vibration of water molecules observed at 1650 cm^{-1} also reducing over time confirmed the densification of the CSH structure. The sharpening and increased intensity of peaks, particularly in the Si-O-(Ca) and Si-O-Si regions, indicated an improvement in structural order, similar to the trends reported in prolonged curing experiments [1,6,10,31].

- *Thermal Characteristic of Day 14 As-Synthesised CSH*

The thermogravimetric analysis (TGA) and differential scanning calorimetry (DSC) thermogram presented in Fig. 3 provided intuition into the thermal stability and decomposition behavior of the calcium silicate hydrate (CSH) sample. The observed thermal behavior of the as-synthesised CSH in this work was consistent with those reported by [21], [11] and [12]. The thermogram revealed thermal behavior which highlighted the hydration, dehydroxylation, carbonation, and stability characteristics of the CSH. The findings were consistent with those reported for calcium silicate hydrates and related materials, supporting the identification of key structural and thermal properties for potential applications [5,33].

- *Morphology and Elemental Constituent of Day 14 CSH*

The SEM micrograph revealed a well-developed network of plate-like and needle-like structures, characteristic of a tobermorite-type CSH phase. These formations suggest significant maturation of the CSH gel over the 14-day period. Tobermorite formation in CSH phases has been widely reported during prolonged curing or hydrothermal conditions [10,31]. The sample showed compact, dense agglomerations, indicating significant polymerization of silicate chains and a reduction in porosity. The dense packing was an indication of possible enhancement in structural stability. Studies have shown that prolonged curing periods lead to reduced porosity and enhanced crystallinity in CSH [13]. The EDX spectrum corroborated the XRF results as it revealed silicon and calcium as the major constituent element in the sample with largely insignificant amount of impurities. Other literature reports showed spectral for CSH that were similar to the spectrum obtained in this work [11,34,35].

V. CONCLUSION AND RECOMMENDATIONS

Calcium silicate hydrate (CSH) was successfully synthesized using precursors such as de-aluminated metakaolin, oyster shells, and calcium hydroxide. The chemical analysis confirmed the high purity of these precursors, with calcium hydroxide exhibiting a CaO content of 98.65 wt% and de-aluminated metakaolin showing a dominant SiO_2 composition of 98.30 wt%. The FTIR spectra demonstrated the progressive development of characteristic functional groups, including Si-O-Si, Si-O(Ca), and O – H bonds, indicating the evolution of the CSH phase over 14 days. The TGA analysis revealed significant thermal stability of the CSH with major weight losses corresponding to dehydration and decarbonation. The SEM micrograph at Day 14 showed a well-formed, dense tobermorite-like structure, indicating a highly polymerized and crystalline morphology, consistent with literature on matured CSH phases. This microstructure suggests enhanced mechanical properties and reduced porosity, making the material suitable for high-performance cementitious applications. The combination of oyster shell-derived calcium hydroxide and silica-rich dealuminated metakaolin as precursors provides a sustainable approach for CSH synthesis, with results demonstrating

ISSN No: -2456-2165 https://doi.org/10.38124/ijisrt/25oct1118

comparable properties to those reported in literature. This study highlights the potential of waste-derived precursors in developing eco-friendly and efficient construction materials.

ACKNOWLEDGEMENTS

Authors would like to express their profound gratitude to ZEOTEC LTD, Ghana for funding this research work.

REFERENCES

[1]. Kumar, A., Walder, B. J., Mohamed, A. K., Hofstetter, A., Rossini, A. J., Scrivener, K., et al., (2017). The Atomic-Level Structure of Cementitious Calcium Silicate Hydrate. *Journal of Physical Chemistry C*, *121*(32), 17188–17196. Retrieved from http://pubs.acs.org.

[2]. Picker, A., Nicoleau, L., Burghard, Z., Bill, J., Zlotnikov, I., Labbez, C., Cölfen, H., et al., (2017). Mesocrystalline calcium silicate hydrate : A bioinspired route toward elastic concrete materials. *Science Advances*, *3*(11), e1701216.

[3]. Kuwahara, Y., Tamagawa, S., Fujitani, T., & Yamashita, H. (2013). A novel conversion process for waste slag: synthesis of calcium silicate hydrate from blast furnace slag and its application as a versatile adsorbent for water purificatio. *Journal of Materials Chemistry A*, *1*, 7199–7210. https://doi.org/10.1039/c3ta11064h.

[4]. Zeng, L., Yang, L., Wang, S., & Yang, K. (2014). Synthesis and Characterization of Different Crystalline Calcium Silicate Hydrate : Application for the Removal of Aflatoxin B1 from Aqueous Solution. *Journal of Nanomaterials*, *2014*, 10. https://doi.org/10.1155/2014/431925.

[5]. Kumar, A., Scrivener, P. K., & Bowen, P. P. (2015). *Synthesis of nano-structured Calcium silicate hydrate Powder Technology Laboratory , École Polytechnique Fédérale de Lausanne EPFL , Switzerland*. *Advanced Materials*. Switzerland.

[6]. Martín-Garrido, Moisés Martínez-Ramírez, Sagrario Pérez, G. G. A. (2016). *Calcium Silicate Hydrate Characterization by Spectroscopic Techniques*. Madrid.

[7]. Zhu, G., Li, H., Wang, X., Li, S., Hou, X., Wu, W., & Tang, Q. (2016). Synthesis of Calcium Silicate Hydrate in Highly Alkaline System. *The American Ceramic Society*,*99*(8),2778–2785. https://doi.org/10.1111/jace.14242.

[8]. Estrada-Flores, S., Martıınez-Lu, evanos A., Bartolo-P´erez, P., Garc´ıa- Cerda, L. A., Flores-Guia, T. E., & Aguilera-Gonz´alez, E. N. (2018). Facile synthesis of novel calcium silicate hydrated- nylon 6/66 nanocomposites by solution mixing method. *RSC Advances*, *8*, 41818-41827. https://doi.org/10.1039/c8ra07116k.

[9]. Shuping, W., Xiaoqin, P., Luping, T., Lu, Z., & Cong, L A N, C. (2018). Influence of Hydrothermal Synthesis Conditions on the Formation of Calcium Silicate Hydrates : from Amorphous to Crystalline Phases. *Journal of Wuhan University of Technology-Mater. Sci. Ed.*, *33*(5), 1150–1158. https://doi.org/10.1007/s11595-018-1947-0.

[10]. Maddalena, R., Li, K., Chater, P. A., Michalik, S., & Hamilton, A. (2019). Direct synthesis of a solid calcium silicate hydrate (C-S-H). *Construction and Building Materials*, *223*, 554-565. https://doi.org/10.1016/j.conbuildmat.2019.06.024.

[11]. Wang, B., Yao, W., & Stephan, D. (2019). Preparation of calcium silicate hydrate seeds by means of mechanochemical method and its effect on the early hydration of cement. *Advances in Mechanical Engineering*, *11*(4), 1–7. https://doi.org/10.1177/1687814019840586.

[12]. Ogur, E., Botti, R., Bortolotti, M., Colombo, P., Vakifahmetoglu, C., & Industriale, I. (2021). Synthesis and additive manufacturing of calcium silicate hydrate scaffolds. *Journal of Materials Research and Technology*, *11*, 1142–1151. https://doi.org/10.1016/j.jmrt.2021.01.090.

[13]. Qi, F., Zhu, G., & Zhang, Y. (2021). Effect of calcium to silica ratio on the synthesis of calcium silicate hydrate in high alkaline desilication solution. *Journal of American Ceramic Society*, *104*(April 2020), 535–547. https://doi.org/10.1111/jace.17440.

[14]. Harris, A. W., Manning, M. C., Tearle, W. M., & Tweed, C. J. (2002). Testing of models of the dissolution of cements – leaching of synthetic CSH gels, *32*, 731-746.

[15]. Chen, J. J., Thomas, J. J., Taylor, H. F. W., & Jennings, H. M. (2004). Solubility and structure of calcium silicate hydrate. *Cement and Concrete Reasearch*, *34*(10), 1499–1519. https://doi.org/10.1016/j.cemconres.2004.04.034.

[16]. Trankle, S., Jahn, D., Neumann, T., Nicoleau, L., Husing, N., & Volkmer, D. (2013). Conventional and microwave assisted hydrothermal syntheses of 11 Å tobermorite. *Journal of Materials Chemistry A*, *1*(35), 10318–10326. https://doi.org/10.1039/c3ta11036b.

[17]. Matsuyama, H. & Young, F. J. (1999). Synthesis of calcium silicate hydrate / polymer complexes : Part. I. *Journal of Materials Research and Technology*, *14*(8), 3379–3388.

[18]. Amuzu, A.C.K., Abandoh, A., Labik, L. k., Puzer, D. B., Gyening, R. O. M., Nkrumah, I., Abavare, E. K. K., & Kwakye-Awuah, B. (2025). Novel Pathway for the Synthesis of High Purity Silica from De-aluminated-metakaolin-derived Sodium Metasilicate Hydrate. *International Journal of Innovative Science and Research*, x(y), a-b. https://doi.org/10.5281/zenodo.12345678.

[19]. Li, J., Zhang, W., Xu, K., & Monteiro, P. J. M. (2020). Fibrillar calcium silicate hydrate seeds from hydrated tricalcium silicate lower cement demand. *Cement and Concrete Reasearch*, *137*(8), 106195. https://doi.org/10.1016/j.cemconres.2020.106195.

[20]. Biagioni, C., Bonaccorsi, E., Merlino, S., & Bersani, D. (2013). Cement and Concrete Research New data on the thermal behavior of 14 Å tobermorite. *Cement and Concrete Research*, *49*, 48–54. https://doi.org/10.1016/j.cemconres.2013.03.007.

[21]. Yu, P. (2022). Thermal dehydration of tobermorite and

ISSN No: -2456-2165 https://doi.org/10.38124/ijisrt/25oct1118

jennite. *Concrete Science and Engineering*, *1*(12), 185–191.

[22]. Woo, S., & Choi, Y.-C. (2023). Synthesis of calcium silicate hydrate nanoparticles and their effect on cement hydration and compressive strength. *Construction and Building Materials*, *407*, 133559.

[23]. Augustyniak, A., Sikora, P., Jablonska, J., Cendrowski, K., John, E., Stephan, D., & Mijowska, E. (2020). The effects of calcium – silicate – hydrate (C – S – H) seeds on reference microorganisms. *Applied Nanoscience*, *10*(12), 4855–4867. https://doi.org/10.1007/s13204-020-01347-5.

[24]. Cristina, L., Alberto, R., Machado, L. B., Aparecida, L., & Motta, D. C. (2019). Industrial Crops & Products Optimization of metakaolin-based geopolymer reinforced with sisal fibers using response surface methology. *Industrial Crops & Products*, *139*(7), 111551. https://doi.org/10.1016/j.indcrop.2019.111551.

[25]. Kwakye-Awuah, B., Abavare, E. K. K., Ntiri-Sefa, B., Nkrumah, I., & Von-Kiti, E. (2021). Synthesis and characterization of geopolymer - zeolites from Ghanaian Kaolin samples by variation of two synthesis parameters. *Journal of Thermal Analysis and Calorimetry*, *146*(5), 18–21. https://doi.org/10.1007/s10973-021-10710-9.

[26]. Lingyu, T., Dongpo, H., Jianing, Z., & Hongguang, W. (2021). Durability of geopolymers and geopolymer concretes : A review. *Reviews on Advanced Materials Science*, *60*(1), 1–14. https://doi.org/10.1515/rams-2021-0002.

[27]. Tijani, J. O., Bankole, M. T., Hussein, A., Oketoye, J. A., & Abdulkareem, A. S. (2019). Influence of Synthesis Parameters in the Preparation of Silicon (IV) Oxide Nanoparticles from Dealuminated Metakaolin and Metakaolin with Na2SiO3. *Journal of Chemical Society of Nigeria*, *44*(6), 1143–1156.

[28]. Bellei, P., Torres, I., & Solstad, R. (2023). Potential Use of Oyster Shell Waste in the Composition of Construction Composites : A Review. *Buildings*, *13*, 1546. https://doi.org/10.3390/buildings13061546.

[29]. Amaechi, P., Sunday, V., & Inderlal, N. (2023). Modified calcium oxide nanoparticles derived from oyster shells for biodiesel production from waste cooking oil. *Fuel Communications*, *14*(January), 100085. https://doi.org/10.1016/j.jfueco.2023.100085,

[30]. Seesanong, S., Seangarun, C., Boonchom, B., & Laohavisuti, N. (2024). Low-Cost and Eco-Friendly Calcium Oxide Prepared via Thermal Decompositions of Calcium Carbonate and Calcium Acetate. *Materials*, *17*, 3875. https://doi.org/10.3390/ma1715387.

[31]. Richardson, I. G. (2008). The calcium silicate hydrates. *Cement and Concrete Reasearch*, *38*(11), 137–158. https://doi.org/10.1016/j.cemconres.2007.11.005.

[32]. Huang, J., Fan, Y., Mejia, S., Hoyos, B., Chandler, M. Q., Peters, J. F., & Pelessone, D. (2019). Preparation of nano-calcium silicate hydrate and its application in concrete Preparation of nano-calcium silicate hydrate and its application in concrete. *Materials and Engineering*, *631* (022052), 0–5. https://doi.org/10.1088/1757-899X/631/2/022052.

[33]. Elghniji, K., Virlan, C., Elaloui, E., & Pui, A. (2018). Synthesis , characterization of SiO 2 supported-industrial phosphoric acid catalyst for hydrolysis of NaBH 4 solution. *Phosphorus, Sulfur, and Silicon and the Related Elements*, *0*(0), 1–16. https://doi.org/10.1080/10426507.2018.1515946.

[34]. Wang, B., Yao, W., & Stephan, D. (2019). Preparation of calcium silicate hydrate seeds by means of mechanochemical method and its effect on the early hydration of cement. *Advances in Mechanical Engineering*, *11*(4), 1–7. https://doi.org/10.1177/1687814019840586.